

Convergence of the nucleation rate for first-order phase transitions

Andreas Ekstedt^{*}

*Department of Physics and Astronomy, Uppsala University, Box 516, SE-751 20 Uppsala, Sweden;
II. Institute of Theoretical Physics, Universität Hamburg, D-22761 Hamburg, Germany
and Deutsches Elektronen-Synchrotron DESY, Notkestr. 85, 22607 Hamburg, Germany*



(Received 23 May 2022; accepted 5 November 2022; published 23 November 2022)

This paper investigates the importance of radiative corrections for first-order phase transitions. While it is known how to incorporate higher-order corrections to the rate, a detailed convergence analysis has not been performed. This paper performs such an analysis, and the results indicate that radiative corrections can be large while retaining perturbativity. To illustrate the calculations, three representative models are considered. Relevant observables are calculated for each model, and the reliability of perturbation theory is discussed.

DOI: [10.1103/PhysRevD.106.095026](https://doi.org/10.1103/PhysRevD.106.095026)

I. INTRODUCTION

A cosmological first-order phase transition is a watershed moment. If such a transition occurred, not only would it leave a trail of gravitational waves [1–4], but it could also explain the observed baryon asymmetry through electroweak baryogenesis [5]. Therefore, with the advent of gravitational-wave cosmology, the community—theoretical and experimental—prepare for upcoming experiments [6–10]. The success of which promises a unique window into the early Universe, and the chance to not only confirm a first-order transition, but to probe the Higgs potential itself [11,12].

Unfortunately, there are significant theoretical uncertainties for nonequilibrium processes like bubble nucleation [13–15]. These uncertainties, in turn, prevent reliable predictions of the gravitational-wave spectrum, which limits any attempt to constrain the underlying physics if a signal is detected.

Therefore, it is crucial to improve computational methods. Although lattice computations [16,17] are preferable, they are slow even for equilibrium observables. This leaves perturbation theory [13,18–21] as the only viable option for studying models with many free parameters.

Methods for including perturbative corrections for bubble nucleation have been developed in [20–24], yet the size of these corrections has not been appreciated nor has the convergence of the perturbative expansion been investigated.

This paper shows that the expansion can converge despite the first perturbative correction being large. This has important consequences for gravitational-wave predictions, and might significantly alter existing results.

II. HIGH-TEMPERATURE CALCULATIONS

Physical quantities are renormalization-scale invariant [13], gauge invariant [18,25], and free from infrared divergences [26,27] in a consistent perturbative expansion.

However, a naive loop expansion does not work at high temperatures. This is because loop corrections are enhanced, which for example leads to thermal mass corrections [28]. In addition, calculations typically contain large logarithms if the relevant energy-scale is much smaller than the temperature.

These issues can be solved by integrating out high-energy fluctuations and working with an effective field theory (EFT). Such a theory describes energy scales relevant to the phase transition, and all temperature dependence is contained in effective couplings [21,28,29].

In particular, the nucleation rate can be calculated within this EFT. Due to the universality of effective field theories, this makes it possible to study an entire class of zero-temperature theories with a single EFT.

III. THE NUCLEATION RATE

Because quantum fields behave classically at high temperatures, it is possible to use classical nucleation theory to calculate the rate of nucleating bubbles [30,31].

In nucleation theory the system overcomes a potential barrier through thermal fluctuations, and the probability to jump over the barrier is controlled by a Boltzmann factor. To be explicit, consider a particle situated at a minima, with a deeper minima located at the other side of a potential barrier. The rate of escape is then controlled by the barrier

^{*}andreas.ekstedt@desy.de

Published by the American Physical Society under the terms of the Creative Commons Attribution 4.0 International license. Further distribution of this work must maintain attribution to the author(s) and the published article's title, journal citation, and DOI. Funded by SCOAP³.

height: $\Gamma \sim e^{-V/T}$. However, in field theory, spatial gradients also contribute to the energy. So instead of the barrier height, the relevant quantity is an action. This action is evaluated on a classical solution to the equations of motion, the bounce [31,32]. In short, this bounce solution describes the nucleation of a true-vacuum bubble.

Take for example a scalar field—the nucleation rate is proportional to

$$\Gamma \propto e^{-S_B}. \quad (1)$$

If we assume that the scalar potential $V(\phi)$ has one minima at $\phi = \phi_{\text{FV}}$, and a deeper minima at $\phi = \phi_{\text{TV}}$, the bounce is given by [32]

$$\begin{aligned} \nabla^2 \phi_B(|\vec{x}|) &= V'[\phi_B(|\vec{x}|)], & \lim_{|\vec{x}| \rightarrow \infty} \phi_B(|\vec{x}|) &= \phi_{\text{FV}}, \\ \vec{\nabla} \phi_B(|\vec{x}|)|_{|\vec{x}|=0} &= 0, \end{aligned} \quad (2)$$

and the bounce action is

$$S_B = \int d^3x \left[\frac{1}{2} (\vec{\nabla} \phi_B)^2 + V[\phi_B] \right]. \quad (3)$$

Note that S_B is three dimensional. Furthermore, as mentioned, we here consider an effective high-temperature theory. This means that all masses and couplings implicitly depend on the temperature, and that we work with an effective three-dimensional theory [20].

Higher-order corrections to the rate come from including fluctuations around the bounce solution. In general these corrections arise from vacuum diagrams in the bounce background. For example, the one-loop result is [30,31]

$$\Gamma \propto \prod_i \det[-\nabla^2 + M_i^2[\phi_B]]^{-1/2} e^{-S_B}. \quad (4)$$

This functional determinant depends on the leading-order bounce through field-dependent masses.¹

Though the determinant is formally subleading, it can be comparable to the exponent. To see when this happens it is useful to rewrite the rate as

$$\Gamma \propto e^{-S_{\text{eff}}[\phi_B]}, \quad S_{\text{eff}} = S_B + S_{1\text{-loop}}, \quad (5)$$

where we have defined the one-loop effective action [33]

$$S_{1\text{-loop}}[\phi_B] = \frac{1}{2} \sum_i \text{Tr} \log [-\nabla^2 + M_i^2[\phi_B]]. \quad (6)$$

¹The rate should be normalized by a corresponding determinant evaluated at $\phi = \phi_{\text{FV}}$, and zero modes should be omitted [22,24,32].

If we consider large bubbles with radius R , the leading-order bounce action scales as $S_B \sim R^2$ [32], while the one-loop action scales as

$$S_{1\text{-loop}} \sim -R^3 \sum_i [(M_i^2[\phi_{\text{TV}}])^{3/2} - (M_i^2[\phi_{\text{FV}}])^{3/2}]. \quad (7)$$

We see that the perturbative expansion breaks down for large R . In addition, Eq. (7) indicates that higher-order corrections are enhanced even for medium-sized bubbles.

Moreover, $S_{1\text{-loop}}$ can be sizeable if the field-dependent mass of a fluctuating particle is parametrically larger than the scalar mass $M_i^2[\phi_B] \gg V''[\phi_B]$. In this case, however, it is often possible to resum large terms by integrating out the heavy particle [20,22,33,34].

So in general our perturbative expansion differs from a strict loop expansion.

To systematically study higher-order corrections, it is then necessary to introduce a power counting. As an example, consider the potential

$$V(\phi) = \frac{1}{2} m_{3d}^2 \phi^2 - \frac{1}{16\pi} g_{3d}^3 \phi^3 + \frac{1}{4} \lambda_{3d} \phi^4. \quad (8)$$

In a gauge theory the cubic term in Eq. (8) arises from vector-boson loops [35]. As such, this potential is said to describe a radiative barrier. While this potential is not applicable to the Standard model, as the Higgs is too heavy, the same potential also appears in scenarios with heavy scalars [36], and it can also describe a real-scalar theory.

At leading order, the effective couplings in Eq. (8) depend on the original zero-temperature couplings schematically as [28]

$$\lambda_{3d} = T\lambda, \quad g_{3d}^2 = Tg^2, \quad m_{3d}^2 = m^2 + aT^2, \quad (9)$$

where a is a function of zero-temperature couplings.

To show how higher-order corrections to the rate can be included, we first consider the radiative-barrier case in an SU(2) model with a doublet scalar. The cubic term in Eq. (8) then comes from integrating out vector bosons. As such, the vector-boson mass must satisfy $\frac{m_H^2}{m_A^2} \sim \frac{\lambda_{3d}}{g_{3d}^2} \sim \frac{\lambda}{g^2} \ll 1$. This encourages us to define the dimensionless couplings

$$x \equiv \frac{\lambda_{3d}}{g_{3d}^2}, \quad y \equiv \frac{m_{3d}^2}{g_{3d}^4}. \quad (10)$$

Where in addition to x , we also use the dimensionless variable y [37]. With these variables, and a field/coordinate rescaling, the potential is

$$V(\phi) = \frac{1}{2} y \phi^2 - \frac{1}{16\pi} \phi^3 + \frac{1}{4} x \phi^4. \quad (11)$$

Now, different minima of $V(\phi)$ correspond to different phases. In Eq. (11) one minimum is at $\phi = 0$, and another at $\phi = \phi_{\min} \neq 0$. Note that a phase transition can first occur when $\Delta V \equiv V(\phi_{\min}) - V(0) = 0$. This motivates us to define the critical mass as the solution of $\Delta V(y_c, x) = 0$ [21,34]. For a specific zero-temperature model it is then possible to find the critical temperature given y_c . But we refrain from doing so to keep the setup general.

Although the two minima overlap at $y = y_c$, the probability for a bubble to nucleate remains insignificant until² $\Gamma \sim e^{-126}$. So we define the nucleation mass as the solution of $S_{\text{eff}}(y_N, x) = 126$. Close to this nucleation mass, the perturbative expansion is organized as

$$S_{\text{eff}} = S_{\text{LO}} + xS_{\text{NLO}} + x^{3/2}S_{\text{NNLO}} + \dots \quad (12)$$

where powers of x denote how the NLO (next-to-leading order) and NNLO (next-to-next-to-leading order) actions scale compared to the LO (leading-order) action.

The above procedure is the same for general potentials. First one should identify a dimensionless combination of couplings to act as perturbative parameters. The rate can then be calculated order-by-order in the effective theory.

IV. SIZE OF HIGHER-ORDER CORRECTIONS

Consider again the radiative barrier. The leading-order action S_{LO} is defined by Eqs. (2), (3), and (11) while S_{NLO} comes from integrating out vector bosons [18,19,22],

$$S_{\text{NLO}} = \int d^3x \left\{ -\frac{11}{32\pi} \frac{(\partial_\mu \phi_B)^2}{\phi_B} + \frac{\phi_B^2}{(4\pi)^2} \left(-\frac{51}{32} \log \frac{\phi_B}{\mu_3} - \frac{63}{32} \log \frac{3}{2} + \frac{33}{64} \right) \right\}, \quad (13)$$

where ϕ_B is the leading-order bounce solution, and we set the renormalization scale $\mu_3 = 1$. The first term is a one-loop self-energy correction, and the second term comes from integrating out vector bosons to two loops.

Finally, S_{NNLO} is given by

$$\frac{1}{2} \{ \text{Tr} \log [-\nabla^2 + M_H^2] + 3 \text{Tr} \log [-\nabla^2 + M_G^2] \}. \quad (14)$$

The first term comes from Higgs bosons, and the second from Goldstone bosons. Their field-dependent masses are given by [34,38]

$$M_H^2 = V''[\phi_B], \quad M_G^2 = \phi_B^{-1} V'[\phi_B]. \quad (15)$$

In the real-scalar model we have neither Goldstone nor vector bosons. So the NLO contribution coincides with the one-loop result,

²There are different definitions of the nucleation temperature/mass in the literature [14,21]. However, using a different definition of the nucleation mass does not qualitatively change the results.

$$S_{\text{NLO}} = \frac{1}{2} \text{Tr} \log [-\nabla^2 + M_H^2]. \quad (16)$$

While S_{NLO} and S_{NNLO} are known for radiative barriers [22,24], their size and effect on observables have not been systematically analyzed. To do such an analysis, we first need to determine when the expansion converges.

To that end we use the result [22,39]

$$S_{\text{LO}} = \kappa \left[7.24 + 5.68\gamma + \frac{10.4}{1-\gamma} + \frac{1.25}{(1-\gamma)^2} \right], \quad (17)$$

where $\kappa = 64\pi^2 y^{3/2}$ and $\gamma = 128\pi^2 xy$.

For the radiative barrier, direct calculations show that both S_{NLO} and S_{NNLO} scale as $(1-\gamma)^{-3}$ when $\gamma \rightarrow 1$.³ This corresponds to $y \rightarrow y_c = \frac{1}{128\pi^2 x}$. In addition, for smaller γ both S_{NLO} and S_{NNLO} are of similar size as S_{LO} unless $\kappa \gg 1$ [22].

There are then two cases when the expansion breaks down; $\kappa \rightarrow 1$ and $\gamma \rightarrow 1$.

To estimate when $\kappa = 1$, note that the nucleation mass is always lower than the critical mass, and because $\kappa \propto y^{3/2}$, we want y to be as large as possible. Putting these observations together, we expect that the expansion breaks down when

$$64\pi^2 y_c^{3/2} = 1 \Rightarrow x = \frac{1}{8\pi^{2/3}} \approx 0.058. \quad (18)$$

This is an upper bound on x that applies to both the radiative-barrier and the real-scalar model; similar bounds appear in other models.

For the real-scalar model one finds that S_{NLO} grows as $(1-\gamma)^{-2}$, so there are no $\gamma \rightarrow 1$ problems. In contrast, for the radiative barrier both S_{NLO} and S_{NNLO} grow as $(1-\gamma)^{-3}$, which means that radiative corrections are larger.

V. OBSERVABLES

The nucleation mass is defined by

$$[S_{\text{LO}} + xS_{\text{NLO}} + \dots]_{y=y_N} = 126. \quad (19)$$

This equation can be solved by expanding y_N in powers of x ,

$$y_N = y_{\text{LO}} + x y_{\text{NLO}} + x^{3/2} y_{\text{NNLO}} \dots \quad (20)$$

The solution to NLO is

$$S_{\text{LO}}|_{y=y_{\text{LO}}} = 126, \quad y_{\text{NLO}} = \left. \frac{S_{\text{NLO}}}{\partial_y S_{\text{LO}}} \right|_{y=y_{\text{LO}}}. \quad (21)$$

³The bubble radius is $R \propto (1-\gamma)^{-1}$.

In general y_{LO} needs to be found numerically, but we can still study some limits analytically. Indeed, from Eq. (17) we see that y_{LO} grows as x^{-1} for large x , and $y_{\text{LO}} \approx 0.048$ for small x . One then finds that κ can not be larger than $\kappa \approx 6.6$, which means that it is not possible to make higher-order corrections arbitrarily suppressed.

Given y_N , we can calculate observables such as the (inverse) phase-transition duration, which is given by [14,21]

$$\tilde{\beta} \equiv \beta_N/H_N \approx \left. \frac{d}{d \log T} S_{\text{eff}} \right|_{y=y_N}. \quad (22)$$

Because our couplings implicitly depend on the temperature through matching relations, we can use the chain rule to express $\tilde{\beta}$ in terms of x and y derivatives of S_{eff} [36]. In addition, since

$$\frac{d}{d \log T} y \gg \frac{d}{d \log T} x, \quad (23)$$

we can approximate [36]

$$\tilde{\beta} \approx \left. \frac{dy}{d \log T} \nabla_y S_{\text{eff}} \right|_{y=y_N}. \quad (24)$$

Expanding everything in powers of x we find to NLO

$$\nabla_y S_{\text{eff}}|_{y=y_N} = \nabla_y S_{\text{LO}} + x[y_{\text{NLO}} \nabla_y^2 S_{\text{LO}} + \nabla_y S_{\text{NLO}}],$$

where all terms are evaluated at $y = y_{\text{LO}}$. Note that $\nabla_y S_{\text{eff}}$ is calculable purely within the effective theory, while $\frac{dy}{d \log T} \sim 4$ depends on the original zero-temperature model.

Therefore, when describing the phase transition, all nontrivial calculations can be performed within the effective theory—the original zero-temperature model only comes in via matching relations.

VI. A DIMENSION-6 OPERATOR

Consider now a model with a leading-order potential

$$V(\phi) = \frac{1}{2} m_{3d}^2 \phi^2 - \frac{1}{4} \lambda_{3d} \phi^4 + \frac{1}{32} c_6 \phi^6. \quad (25)$$

This model is relevant when effective operators are added to the Standard Model [21]: we consider this to be the case here. That is, neglecting the hypercharge coupling, we consider an $SU(2)$ gauge theory with a doublet scalar. The three dimensional c_6 coupling is related to the zero-temperature one (at leading order) via $c_6 = T^2 c_{6,4d}$.

To study this model it is useful to introduce the dimensionless coupling

$$y = \frac{m_{3d}^2}{\lambda_{3d}^2}. \quad (26)$$

At leading order everything depends on y and c_6 ; both scalars and vector-bosons contribute at NLO according to Eq. (6). These contributions must be calculated numerically [22], but we note that the vector-boson contribution grows as $x^{-3/2}$ for small x , where x was defined in Eq. (10).

The tree-level action can be approximated by [22]

$$S_{\text{LO}} = \sqrt{y} \left[1.76 - 0.142\gamma + \frac{12.6}{(1-\gamma)} + \frac{4.19}{(1-\gamma)^2} \right], \quad (27)$$

where $\gamma = c_6 y$. As before, we can determine y_N and $\tilde{\beta}$ in powers of c_6 and x .

Following the same arguments as for the radiatively-induced potential, we expect that perturbation theory becomes unreliable when $c_6 \gtrsim 1$. However, because the NLO action grows as $x^{-3/2}$ for small x , this bound is modified to $c_6 \gtrsim x^3$.

There is also an absolute lower bound on x regardless of the value of c_6 . This is because y_N can not be arbitrarily large. Indeed, using Eq. (27) we see that y_N is largest when $\gamma = 0$, which corresponds to $y_{\text{LO}} \approx 46$, and because the leading-order action scales as \sqrt{y} , it is not possible to consider arbitrarily small values of x . Numerically, one finds that perturbation theory does not work for x smaller than $x \sim 10^{-1}$.

For smaller x we need to integrate out the vector bosons; to leading order this will generate a cubic term in the tree-level potential.

VII. RESULTS

The radiatively-induced potential is defined by Eq. (8), and the results are shown in Fig. 1. We see that as the nucleation mass decreases—meaning a weaker transition—perturbation theory breaks down. This is expected because weak transitions are generally nonperturbative [16,37,40], yet this breakdown occurs already at $x \approx 0.02$, instead of the bound derived in Eq. (18). This is because S_{NLO} is numerically large, and since both S_{NLO} and S_{NNLO} are enhanced for large bubbles. Note that radiative corrections are large even for smaller x where the expansion is expected to perform well. Indeed, the NLO result for $\nabla_y S_{\text{eff}}$, and thus $\tilde{\beta}$, is roughly a factor of two smaller than the leading-order result. Still, there is not another large jump once S_{NNLO} is included. This indicates that higher-order corrections can be large without invalidating the perturbative expansion.

Radiative corrections are smaller for the real-scalar model as is shown in Fig. 2. In this model the expansion gets worse around $x \approx 0.05$ as expected from Eq. (18). The modest size of the NLO correction stems from that the Higgs mass is equal in the broken and true minima; which coupled with Eq. (7), shows that there is no (large-bubble) R^3 enhancement.

The results for a Standard Model-like potential with an effective ϕ^6 operator are shown in Fig. 3. The results

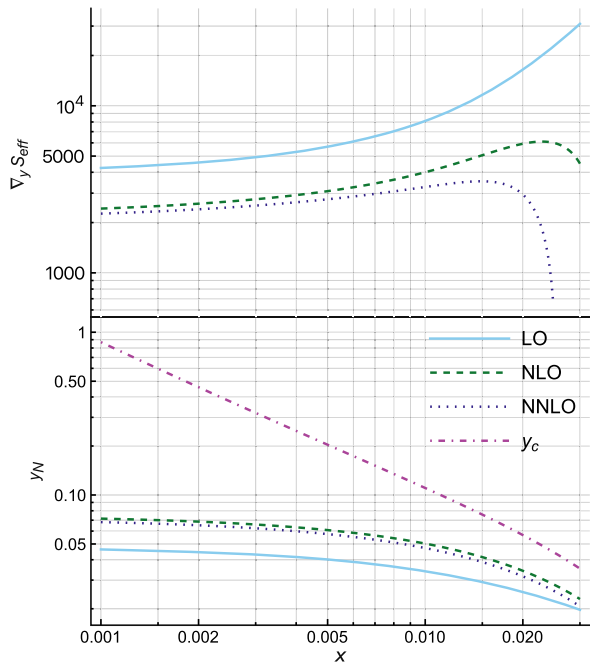


FIG. 1. Results for the radiative barrier described by the potential in Eq. (8); assuming a SU(2) gauge theory with a doublet scalar. The lower plot shows the nucleation mass y_N as a function of x . The critical mass (to NNLO) is shown for comparison. The upper plot shows $\nabla_y S_{\text{eff}} \propto \tilde{\beta}$ at the nucleation mass.

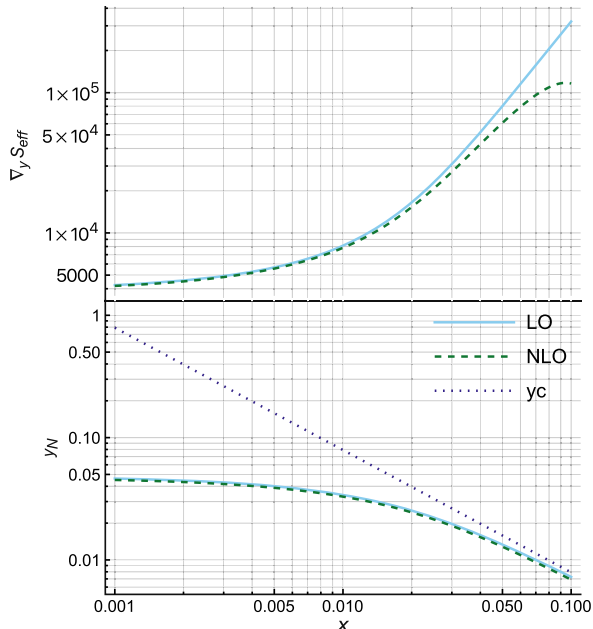


FIG. 2. Results for the real-scalar model described by the potential in Eq. (8). The lower plot shows the nucleation mass y_N as a function of x . The critical mass (to NLO) is shown for comparison. The upper plot shows $\nabla_y S_{\text{eff}} \propto \tilde{\beta}$ at the nucleation mass.

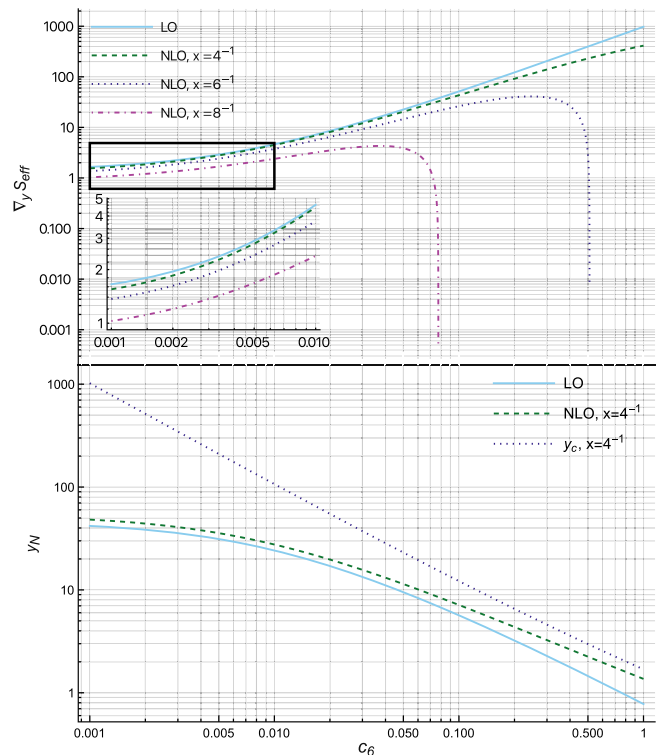


FIG. 3. Results for the potential in Eq. (25); assuming a SU(2) gauge theory with a doublet scalar. The lower plot shows the nucleation mass y_N as a function of c_6 with $x = 4^{-1}$. The critical mass (to NLO) is shown for comparison. The upper plot shows $\nabla_y S_{\text{eff}} \propto \tilde{\beta}$ at the nucleation mass.

indicate that the expansion breaks down for small x . This is because S_{NLO} grows as $x^{-3/2} \sim \lambda_{3d}^{-3/2}$, which pushes the range of validity to small c_6 values; $c_6 \lesssim x^3$.

Interestingly, even when the expansion appears reliable, radiative corrections can be quite large if $x \ll 1$. Although, it should be stressed that we have only calculated the rate to NLO for this model, and it is necessary to include two-loop contributions to ensure that the expansion converges.

Moreover, perturbation theory might still work for smaller x if vector-bosons are integrated out. This would give a cubic term in the leading-order potential, akin to Eq. (8). Higher-order corrections should then be more well-behaved even if x is small. They can still be large, though, as indicated by the radiative-barrier case in Fig. 1.

Finally, note that the nucleation mass is more well-behaved than $\tilde{\beta}$; this is because large radiative corrections cancel due to the ratio in Eq. (21).

VIII. CONCLUSION

Higher-order corrections to the rate have been calculated previously [22–24], yet a convergence analysis has not been performed. Doing such an analysis, we find that radiative corrections to the nucleation rate can be large. In particular, by using a strict perturbative expansion, this

paper calculates the size of these corrections for a variety of models. The calculations indicate that higher-order corrections are important, and should be included when studying extensions of the Standard Model. Even when perturbation theory is reliable, observables can change by a factor of 2 once NLO corrections are included.

Our results also indicate that it is not possible to make higher-order corrections arbitrarily suppressed for the models considered. This does not necessarily mean that perturbation theory is inadequate, but it does encourage caution when estimating the size of higher-order corrections to the rate.

In addition, this work illustrates the synergy between classical nucleation theory and effective high-temperature field theories [20]. Indeed, all nonequilibrium effects can be calculated within the effective theory, while temperature dependence is captured by effective couplings.

For the radiative-barrier model, it is found that perturbation theory breaks down when $x \approx \frac{\lambda}{g^2} \sim 0.02$. This should be contrasted with $x \approx 0.1$, which is the endpoint of the first-order transition [40,41]. This means that perturbation theory only works in a narrow parameter-range for the radiative-barrier model.

Moreover, the results [see Eq. (7)] indicate that perturbation theory converges slowly in the large-bubble limit.

A possible solution is to resum these large R corrections into an effective theory as suggested by [20].

For future work it would be interesting to confirm that the calculations converge for radiative barriers. This would require three-loop calculations, and would be the final calculable contribution due to the Linde problem [42].

Furthermore, the methods of this paper can be applied to models with two-step transitions, like for example singlet/triplet extensions of the Standard Model [11,43,44]. Similar to the models studied in this paper, radiative corrections are expected to be sizeable for such extensions.

ACKNOWLEDGMENTS

The author would like to thank Philipp Schicho, Oliver Gould, and Tuomas V.I. Tenkanen for insightful discussions and for a critical read-through of the paper. During the completion of this paper the author was made aware of similar methods used in the contemporary paper [17]. This work has been supported by the Deutsche Forschungsgemeinschaft under Germany's Excellence Strategy—EXC 2121 Quantum Universe—390833306; and by the Swedish Research Council, Project No. VR:2021-00363.

-
- [1] M. Hindmarsh, S. J. Huber, K. Rummukainen, and D. J. Weir, *Phys. Rev. D* **96**, 103520 (2017).
 - [2] V. Vaskonen, *Phys. Rev. D* **95**, 123515 (2017).
 - [3] C. Grojean and G. Servant, *Phys. Rev. D* **75**, 043507 (2007).
 - [4] F. Giese, T. Konstandin, K. Schmitz, and J. van de Vis, *J. Cosmol. Astropart. Phys.* **01** (2021) 072.
 - [5] V. A. Kuzmin, V. A. Rubakov, and M. E. Shaposhnikov, *Phys. Lett.* **155B**, 36 (1985).
 - [6] Z. Arzoumanian *et al.* (NANOGrav Collaboration), *Astrophys. J. Lett.* **905**, L34 (2020).
 - [7] P. Amaro-Seoane *et al.* (LISA Collaboration), [arXiv:1702.00786](https://arxiv.org/abs/1702.00786).
 - [8] S. Kawamura *et al.*, *Classical Quantum Gravity* **28**, 094011 (2011).
 - [9] W.-H. Ruan, Z.-K. Guo, R.-G. Cai, and Y.-Z. Zhang, *Int. J. Mod. Phys. A* **35**, 2050075 (2020).
 - [10] Y. A. El-Neaj *et al.* (AEDGE Collaboration), *Eur. Phys. J. Quantum Technol.* **7**, 6 (2020).
 - [11] L. S. Friedrich, M. J. Ramsey-Musolf, T. V. I. Tenkanen, and V. Q. Tran, [arXiv:2203.05889](https://arxiv.org/abs/2203.05889).
 - [12] M. J. Ramsey-Musolf, *J. High Energy Phys.* **09** (2020) 179.
 - [13] O. Gould and T. V. I. Tenkanen, *J. High Energy Phys.* **06** (2021) 069.
 - [14] C. Caprini *et al.*, *J. Cosmol. Astropart. Phys.* **03** (2020) 024.
 - [15] H.-K. Guo, K. Sinha, D. Vagie, and G. White, *J. High Energy Phys.* **06** (2021) 164.
 - [16] G. D. Moore and K. Rummukainen, *Phys. Rev. D* **63**, 045002 (2001).
 - [17] O. Gould, S. Güyer, and K. Rummukainen, [arXiv:2205.07238](https://arxiv.org/abs/2205.07238).
 - [18] J. Hirvonen, J. Löfgren, M. J. Ramsey-Musolf, P. Schicho, and T. V. I. Tenkanen, *J. High Energy Phys.* **07** (2022) 135.
 - [19] J. Löfgren, M. J. Ramsey-Musolf, P. Schicho, and T. V. I. Tenkanen, [arXiv:2112.05472](https://arxiv.org/abs/2112.05472).
 - [20] O. Gould and J. Hirvonen, *Phys. Rev. D* **104**, 096015 (2021).
 - [21] D. Croon, O. Gould, P. Schicho, T. V. I. Tenkanen, and G. White, *J. High Energy Phys.* **04** (2021) 055.
 - [22] A. Ekstedt, *Eur. Phys. J. C* **82**, 173 (2022).
 - [23] G. V. Dunne and H. Min, *Phys. Rev. D* **72**, 125004 (2005).
 - [24] J. Baacke and V. G. Kiselev, *Phys. Rev. D* **48**, 5648 (1993).
 - [25] W. Buchmüller, Z. Fodor, and A. Hebecker, *Phys. Lett. B* **331**, 131 (1994).
 - [26] M. Laine, *Phys. Lett. B* **335**, 173 (1994).
 - [27] M. Laine, *Phys. Rev. D* **51**, 4525 (1995).
 - [28] K. Kajantie, M. Laine, K. Rummukainen, and M. E. Shaposhnikov, *Nucl. Phys.* **B458**, 90 (1996).
 - [29] K. Farakos, K. Kajantie, K. Rummukainen, and M. E. Shaposhnikov, *Nucl. Phys.* **B425**, 67 (1994).
 - [30] J. S. Langer, *Ann. Phys. (N.Y.)* **54**, 258 (1969).
 - [31] A. D. Linde, *Nucl. Phys.* **B216**, 421 (1983).
 - [32] S. R. Coleman, *Phys. Rev. D* **15**, 2929 (1977).
 - [33] E. J. Weinberg, *Phys. Rev. D* **47**, 4614 (1993).

- [34] A. Ekstedt, O. Gould, and J. Löfgren, *Phys. Rev. D* **106**, 036012 (2022).
- [35] P. B. Arnold and O. Espinosa, *Phys. Rev. D* **47**, 3546 (1993).
- [36] O. Gould, J. Kozaczuk, L. Niemi, M. J. Ramsey-Musolf, T. V. I. Tenkanen, and D. J. Weir, *Phys. Rev. D* **100**, 115024 (2019).
- [37] K. Kajantie, M. Laine, K. Rummukainen, and M. E. Shaposhnikov, *Nucl. Phys.* **B466**, 189 (1996).
- [38] A. Ekstedt and J. Löfgren, *J. High Energy Phys.* 12 (2020) 136.
- [39] M. Dine, R. G. Leigh, P. Y. Huet, A. D. Linde, and D. A. Linde, *Phys. Rev. D* **46**, 550 (1992).
- [40] M. Gurtler, E.-M. Ilgenfritz, and A. Schiller, *Phys. Rev. D* **56**, 3888 (1997).
- [41] K. Rummukainen, M. Tsypin, K. Kajantie, M. Laine, and M. E. Shaposhnikov, *Nucl. Phys.* **B532**, 283 (1998).
- [42] A. D. Linde, *Phys. Lett.* **96B**, 289 (1980).
- [43] L. Niemi, P. Schicho, and T. V. I. Tenkanen, *Phys. Rev. D* **103**, 115035 (2021).
- [44] N. F. Bell, M. J. Dolan, L. S. Friedrich, M. J. Ramsey-Musolf, and R. R. Volkas, *J. High Energy Phys.* 05 (2020) 050.